International Journal of Botany Studies
ISSN: 2455-541X; Impact Factor: RJIF 5.12
Received: 28-12-2020; Accepted: 29-01-2021: Published: 05-02-2021
www.botanyjournals.com
Volume 6; Issue 1; 2021; Page No. 432-437

Biosynthesis of zinc oxide nanoparticles using seed extract of *Moringa oleifera* and its effect on azo dye degradation

Veena M Sathiyabama
Department of Botany, School of Life Sciences, Bharathidasan University, Tiruchirappalli, Tamil Nadu, India

Abstract
Synthetic dyes are widely used in textile, paper, food, cosmetics and pharmaceutical industries as above the textile industry was the largest consumer. Azo dyes are the largest group among all other synthetic dyes used in textile industry. Textile dyeing and finishing processes generate a large amount of dye contaminating the main sources of water; it's the big bang pollution problems worldwide. Nanoparticles can be synthesized by using green synthesis methodologies with microbes and plant extracts. Under the favorable conditions, size and surface of nanoparticles can be easily altered to achieve Eco friendly degradation of azo dyes. Nanotechnology is recognized as the study of particle with a minimum of one dimension in nanometers. This work is based and focused on the green synthesis of ZnO nanoparticles using the seed extract of *Moringa oleifera* L. Characterization of Zinc nanoparticles was done by UV-Visible spectrophotometer for its Surface Plasmon resonance, SEM for morphologies, XRD and FTIR for its structure and DLS for determination of the size. The synthesized nanoparticles was evaluated for its efficiency in reducing the azo dyes.

Keywords: green synthesis, ZNO nanoparticles; *Moringa oleifera*, azo dye, degradation

Introduction

Dyes are generally organic chemicals, these are important for its colouring properties in various industries. Dyes are classified by

1. The chemical structures – style of chromophore groups present in dye which are named as groups – like azo dyes, anthraquinone dyes and phthalocyanine dyes etc. and
2. Their usage or application method as disperse dyes for polyester and reactive dyes for cotton (Singh *et al.*, 2012) [21].

Azo (monoazo, diazo, triazo and polyazo), anthraquinone, triarylmethane and phthalocynine dyes are main groups of dyes. Azo dyes absorb light within the visible region thanks to their chemical structure, which is characterized by one or more azo bonds (-N=N-) (Chang *et al.*, 2001) [4]. Globally, 2.8×105 a lot of textile dyes are poured into water ecosystem per annum (Jin *et al.*, 2007). Azo dyes are the foremost common (more than 3000 different varieties) of all textile dyes produced thanks to their easier biosynthesis, chemical stability. Therefore the diversity of colours available as compared to natural dyes (Chang *et al.*, 2004) [3]. About 80% of azo dyes are employed in the dyeing process of textile industries. They're widely employed in the textile, leather, food, paper, cosmetics and pharmaceutical industries. It's been estimated that about 10-15% of the dyes utilized in dying process goes unbound with the textile fibres and are discharged into the environment (Asad *et al.*, 2007) [1]. Release of dye containing effluent derived from various industrial practices into water bodies and surrounding industrial areas is of major concern (Mugdha and Usha, 2012) [16] which have several adverse effects on various aquatic life including decreased aquatic photosynthesis, ability to exhaust dissolved oxygen and toxic effect on flora, fauna and also to humans. Presence of dyes within the textile effluent causes an unpleasant appearance by imparting the colour and also their breakdown products (colorless amines) are toxic, carcinogenic and mutagenic (Xu *et al.*, 2005) [24].

Azo dyes are present in the textile effluent are a major problem due to their toxic nature. Azo dyes having a nitro group that are proved to be mutagenic in nature (Chung and Cerniglia, 1992) [5] and after breakdown they generate toxic products such as 1, 4-phenylenediamine, o-tolidine etc. (Rosenkranz and Kolpman, 1990). Also it is reported that, sulfonated azo dyes pretended less or no mutagenic effect as compared to unsulfonated azo dyes (Jung *et al.*, 1992) [12]. A unique aromatic amine, 3-methoxy-4-aminoazobenzene, has been found to be potent hepato carcinogen in rats and a potent mutagen in bacteria (Ferraz *et al.*, 2011) [9]. Biological treatment for the decolorization and degradation of azo dyes has advantages and disadvantages. Therefore, it is necessary to search for more active and versatile enzymes, microorganisms and techniques with high stability and low cost that is suitable to meet the requirements of textile industry wastewater treatment. In the last few years various nanoparticles are widely used for the degradation of azo dyes. Nanotechnology is a very promising technique, having an important role in improvement of manufacturing technologies, telecommunications, electronics, health and even in environmental remediation (Gross, 2001; Kim *et al.*, 2005; Moore, 2006) [10, 13, 15]. Recently, nanomaterials (NMs) have been used as efficient, cost effective and eco-friendly alternative to existing treatment materials, from the standpoints of both resource conservation and environmental remediation (Dimitrov, 2006; Dastjerdi and Montazer, 2010) [8, 6]. With unique physical and chemical properties nanomaterials have a remarkable potential for toxic contaminant removal. Nanotechnology offers production and utilization of a different range of NMs, with size ranging from 1 to 100 nm and exhibit unique properties

which are not found in bulk-sized materials (Stone *et al.*, 2010; Wang *et al.*, 2010) [22, 23]. Bokare *et al.*, 2008 [2] they investigated degradation of Orange G, a monoazo dye, in aqueous solutions by using Fe-Ni bimetallic nanoparticles. Dehghani and Mahdavi 2015 [7] performed experiments in a batch photo reactor on synthetic wastewater with concentrations of 0.5, 1.0, 1.5 and 2 mg l-1. The study investigated the effects of factors such as irradiation time, a dose of catalyst, initial dye concentration and pH on decolorization extent of Acid Red 4092 dye by the photo catalytic process in the presence of zinc oxide nanoparticles. Sharma *et al.*., 2016 have studied decolorization and degradation of Methyl Red by suspended and immobilized cells of *Aeromonas jandaei* strain SCS5 under anaerobic and aerobic conditions. The complete decolorization of Methyl Red at a concentration of 100 mg l-1 by *A. jandaei* strain SCS5 was recorded within 6 h for both anaerobic and aerobic suspended cultures, but the decolorization rate was faster in acidic than basic conditions.

The present study were conducted with the *Moringa oleifera* medicinal plant seeds for the green synthesis of zinc oxide NPs and their photocatalytic activity against the degradation of Azo dyes such as methyl orange and congo red with following objectives.

Materials and Methods

Synthesis of Zinc oxide Nanoparticle

5 grams of *Moringa oleifera* seeds were washed thoroughly with distilled water and heated for 40 min in 100 ml of distilled water at 50^{O} C. Then the extract was filtered with Whatman 41 filter paper. Zinc Nitrate hexahydrate [Zn (NO3)2·6H2O] (Merck, Mumbai) was used as a precursor for the synthesis of ZnO nanoparticles from *M. oleifera*. 1mM Zinc nitrate solution was prepared using double distilled water and stored in refrigerator at 4 °C for further use. The *M. oleifera* extracts were used to reduction of metal ions in to metallic oxide nanoparticles. Three boiling tubes were used to synthesize ZnO nanoparticles, one containing 10 ml of 1mM Zinc nitrate solution as reference, and the second one containing 10 ml of aqueous plant extract and the third tube contained 5 ml of 1 mM Zinc nitrate solution and 5 ml of plant extracts as reaction medium and incubated at room temperature. To observe the visual color change, the reaction medium was boiled for 20 min at the temperature of 60 °C. The test solution from the third tube was centrifuged at 5000 rpm for 20 min to obtain the pellet. Supernatant is discarded and the pellet is dissolved in double distilled water. The pellets obtained were washed and obtained pellet was then lyophilized.

Characterization Techniques

UV-vis spectra analysis

The formation of Zn oxide nanoparticles were analyzed by measuring the wave length of reaction mixture in the UV-vis spectrum of the PerkinElmer spectrophotometer at a resolution of 1 nm (from 300 to 600 nm) in 2 ml quartz cuvette with 1 cm path length

SEM analysis

The Morphological characterization of the samples was done using JEOL Jsm-6480 LV for SEM analysis. The samples were dispersed on a slide and then coated with platinum in an auto fine coater.

DLS Particle size

The size distribution or average size of the synthesized Zn oxide NPs were determined by dynamic light scattering (DLS) and zeta potential measurements were carried out using DLS (Malvern, UK). For DLS analysis the samples were diluted 10 folds using 0.15M PBS (pH 7.4) and the measurements were taken in the range between 0.1 and 10,000 nm.

FT-IR analysis

The characterization of functional groups on the surface of ZnONPs by plant extracts were investigated by FTIR analysis (Shimadzu) and the spectra was scanned in the range of 4000– 400 cm−1 range at a resolution of 4 cm−1. The samples were prepared by dispersing the AgNPs uniformly in a matrix of dry KBr, compressed to form an almost transparent disc. KBr was used as a standard analyse the samples.

XRD analysis

XRD measurements of the reduced ZnONPs perform were recorded on X-ray diffractometer (x'pert pananalytical) instrument operating at a voltage of 40 kV and current of 30 mA with Cu K (α) radiation to determine the crystalline phase and material identification.

Preparation of Azo dye

The Azo dye methyl orange and Congo red was purchased from Merck, India. One gram of Azo dyes dissolved in 1000ml of double distilled water. The dye concentration was 0.1%. Further the prepared dye stored for further studies.

Dye degradation by UV Photo catalytic method

The photocatalytic activity of the biosynthesized ZnO NPs was investigated via the photocatalytic degradation of methylene blue (MB) and Congo red (CR) (dyes normally resistant to biodegradation). The photocatalytic experiments were performed under UV light (24 W UV lamp, 360 nm) irradiation. The photocatalytic decomposition of MB and CR solution (50 ppm) by plant based ZnO NPs as a photocatalyst (0.02 g) was performed in a 100 mL beaker at 35 ◦C under UV irradiation and continuous stirring to achieve the homogeneity of the solution. Absorbance was measured with a UV-Vis spectrophotometer. Effect of ZnO NPs dosages on degradation of MB and CR was studied with various time intervals from 0 mins to 200 mins in 25 mins increments. The degradation rate of MB was calculated as follow [Meena *et al.*, 2016]:

Degradation %= (A0 □ A)/A0 _ 100 (3)

Where A0 is the absorbance at t = 0 min and A is the absorbance after treatment.

Results and Discussion

The preliminary results revealed that the color of the sample changed from pale white to brown color which was due to the reduction of zinc ions into zinc oxide nanoparticle that occurred due to the surface plasmon resonance phenomenon.

UV-visible analysis

The reduction of zinc metal ions to zinc oxide nanoparticles in the reaction medium was preliminarily analyzed using

UV-Vis Spectrophotometer between 200 to 700 nm. The UV-Visible spectroscopic analysis of ZnO nanoparticles from *M. oleifera* was confirmed by the strong absorption spectra at 272 nm.

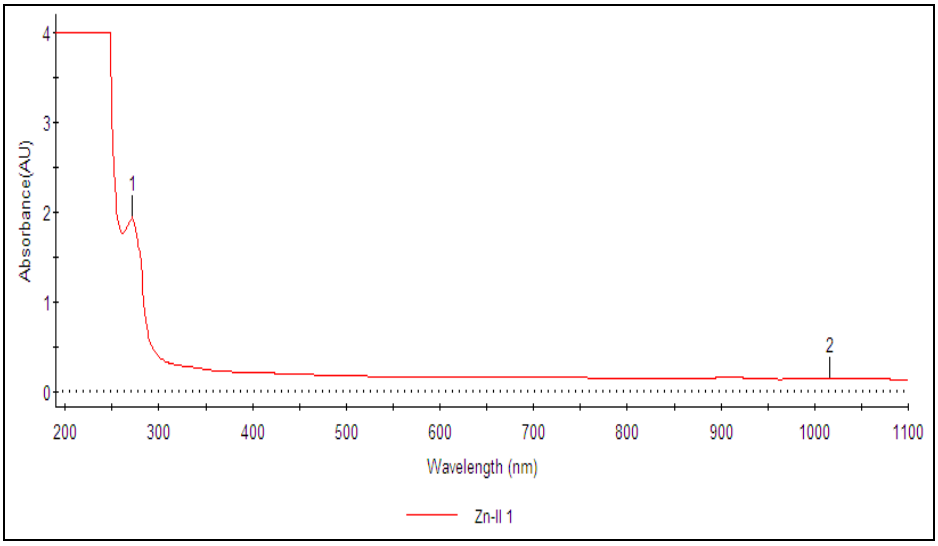

Fig 1: UV spectroscopy analysis of nanoparticles synthesised from *Moringa oleifera*

FTIR analysis

The surface chemistry of the nanoparticles synthesized was revealed by the appearance in the FTIR spectra of IR bands at 3456.30, 2983.78, 2093.40, 1637.20, 1405.81, 1253.74, 1182.00 and 651.80 cm−1 and by the peaks which correspond to various groups (Figure 2). The peak around 1320–1000 cm-1 leads to C-O stretching alcohols, carboxylic acids, esters and ethers. Here the C-O stretching alcohols, carboxylic acids, esters, ethers which show the peak at 1253.74 cm^{-1}.1500-1400 cm^{-1}leads to C-C stretch (in-ring) aromatics. Here the C-C stretch (in-ring) aromatics show the peak at 1405.81 cm^{-1}. The peak around 1650–1580 cm^{-1} leads to N–H bend primary amines. Here the observed peak is 1637 cm^{-1} leads to N–H bend primary amines. Here the observed peak is 3456.30cm^{-1} leads to N-H stretching for primary, secondary amines, amides. Thus, the synthesized ZnO nanoparticles are surrounded by proteins and metabolites like terpenoids with the attachment of the various functional groups. The FTIR analysis confirmed the presence of carbonyl groups from the amino acid residues and proteins has the stronger capability to bind the metal designating the proteins which can probably from the metal nanoparticles, i.e. capping of zinc oxide nanoparticles which suggests the biological molecules has the capability to perform dual functions of formation and stabilization of ZnO nanoparticles. In 2019, Abbasi *et al.*, also stated the peaks obtained in the region of 3286 to 3290 and 1051 to 1058 cm−1 in all four FTIR spectrums are attributed to C–H and C–O–C stretching and peaks at 2360 cm−1 are due to C=C stretching vibrations using *M. oleifera*. Our findings are supported by some previous reports (Sangeetha *et al.*, 2011; Sagar Raut *et al.*, 2013) [19, 18].

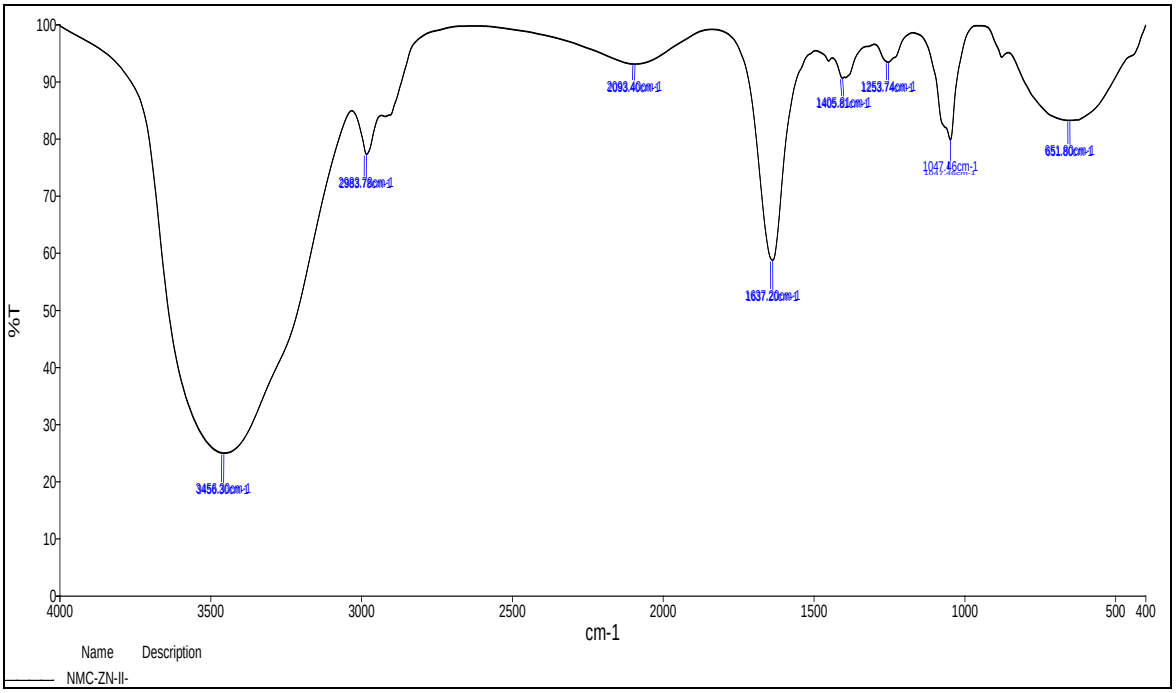

Fig 2: FTIR analysis of nanoparticles synthesised from *Moringa oleifera*

XRD analysis

The XRD pattern of the ZnONPs synthesized via *Moringa oleifera* ethanol extract was compared and interpreted using standard data. The major peaks at 38°, 46°, 65°, and 78° (2θ values) correspond to the reflections from the (111), (200), (220), and (311) planes, respectively, and confirm the crystalline phase of the AgNPs. The polycrystalline nature of extract-synthesized AgNPs can be inferred from the fact that the XRD data suggest smaller crystallite sizes than the particle sizes observed in SEM images (Figure 3).

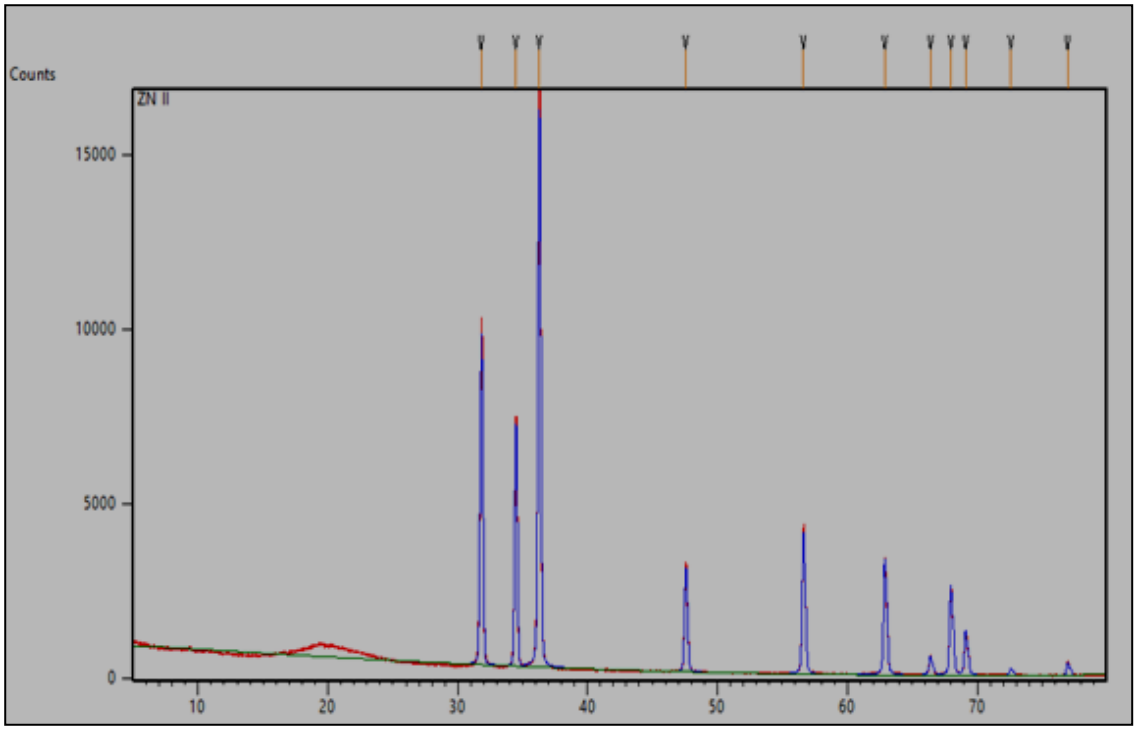

Fig 3: XRD analysis of nanoparticle synthesised from *M. oleifera*

FE-SEM

The 3D structure of zinc oxide nanoparticles has been elucidated using SEM image. The SEM image revealed that zinc oxide nanoparticles formation was due to hydrogen bond and electrostatic interactions between the bioorganic capping molecules bound to the zinc nanoparticles. (Figure 4). It was shown that relatively cuboid and uniform ZnO NPs were found with diameter of 67 to 95nm. The nanoparticles synthesised from *Moringa oleifera* seed extract were observed as cylindrical in nature as showed in Figure 4.

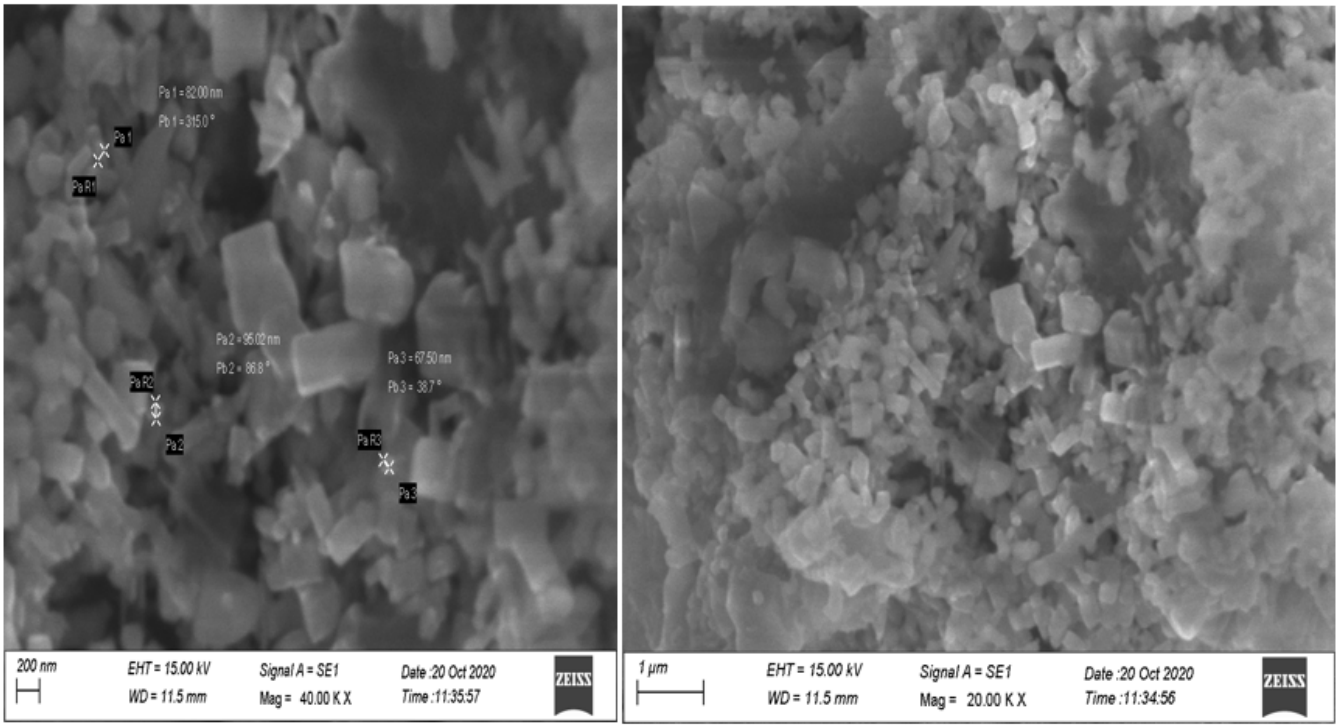

Fig 4: SEM analysis of ZO nanoparticle synthesised from *Moringa oleifera*

DLS Particle size and zeta potential analysis

Zeta potential values provide an indirect measurement of the net charge on the nanoparticle (NP) surface. Zeta potential in general represents the surface charge and functionality and is a prerequisite for determining the material's isoelectric point and the ZnO NPs showed a potential of -35 mV for ZnO Nps. Thus DLS data showed that single peak is at 16 nm (100%) and Polydispersity Index is 0.452. At the temperature of 25ºC the Polydispersity Index value is 0.452 on 1615.5 nm in diameter (Figure 5).

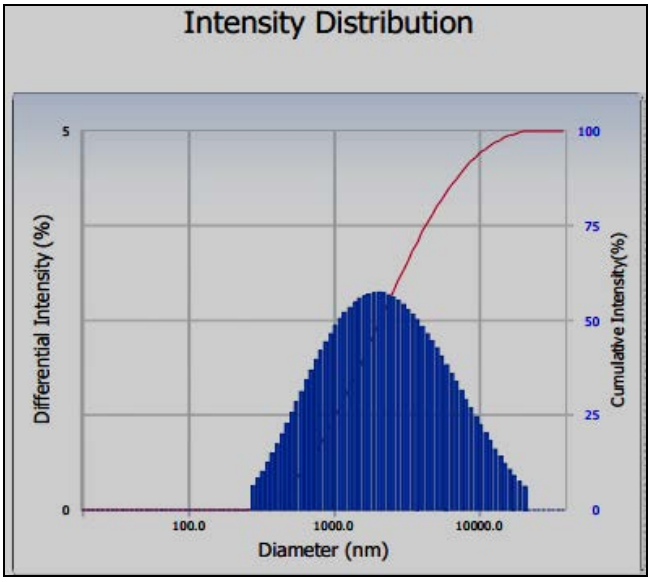

Fig 5: Size distribution and Zeta potential of ZO nanoparticles mediated by *M. oleifera*

Photocatalytic Tests

Methylene Blue and Congo red is an aromatic heterocyclic chemical compound. The spectrum of the dyes solution in aqueous medium shows characteristics peaks at 375nm (Methylene blue) and 360, 362nm (Congo red) respectively. Then after several time intervals in the presence of ZO NPs suspension the absorbance decreases from 375 and 360nm in presence of visible light illumination is presence of ZO NPs proved that the synthesized nanoparticles have significant photo degradation ability (Figure 6, 7).

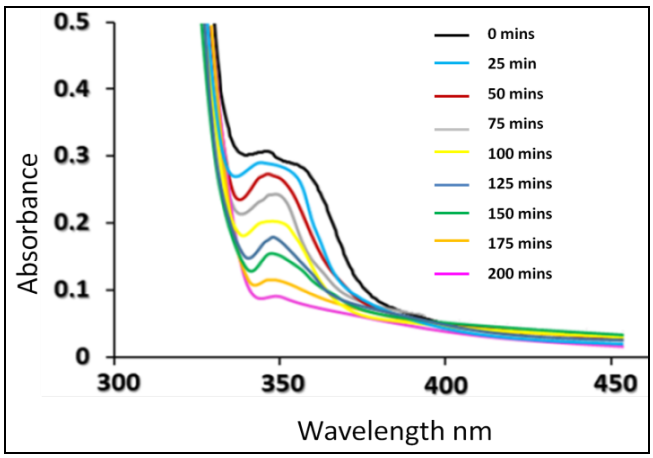

Fig 6: Photocatalytic activity - Degradation of methylene blue

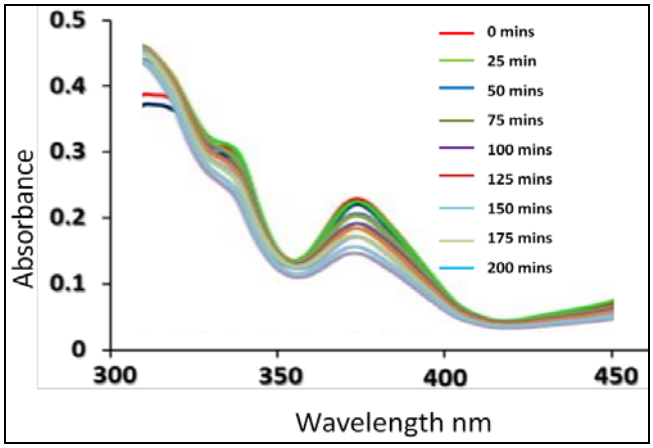

Fig 7: Photocatalytic activity - Degradation of congo red

Conclusion

Zinc oxide nanoparticles were effectively synthesized by using green synthesis method using *Moringa oleifera* seed extract. The UV-Vis spectroscopic study shows the Plasmon resonance property, confirmed the reduction of metal ion and formation of nanoparticle with plasma resonance peak at 272. FTIR measurements were carried out to categorize the possible biomolecules responsible for capping and efficient stabilization of the metal nanoparticles synthesized by the *M. oleifera*. The XRD study confirms the structure of ZnO nanoparticles and also the formation of narrow peak with the Bragg's angle of 2θ=102˚ suggests the crystalline nature and wurtzite structure of ZnO nanoparticles. At the Bragg's angle of 2θ=100˚ suggests the face centered cubic nature of the ZnO nanoparticles. Stabilization of the nanoparticles occurs by some capping agents which are confirmed by the sharp peaks. At the temperature of 25ºC the Polydispersity Index value is 0.452 on 1615.5 nm in diameter. The scattering and refractive index is 29675 and 1.3328 cps. Photocatalytic activity of Methylene Blue and Congo red showed the spectrum of the dyes solution in aqueous medium shows characteristics peaks at 375nm (Methylene blue) and 360, 362nm (Congo red) respectively. Then after several time intervals in the presence of ZONPs suspension the absorbance decreases from 375 and 360nm in presence of visible light illumination is presence of ZONPs proved that the synthesized nanoparticles have significant photo degradation ability.

Acknowledgement

The authors thank DST-PURSE, RUSA Phase 2, Bharat Hidasan University for support.

References

1. Asad S, Amoozegar MA, Pourbabaee A, Sarbolouki MN, Dastgheib SMM. Decolorization of textile azo dyes by newly isolated halophilic and halotolerant bacteria. Bioresource technology. 2007; 98(11):2082-2088.
2. Bokare AD, Chikate RC, Rode CV, Paknikar KM. Iron-nickel bimetallic nanoparticles for reductive degradation of azo dye Orange G in aqueous solution. Applied Catalysis B: Environmental. 2008; 79(3):270-278.
3. Chang JS, Chen BY, Lin YS. Stimulation of bacterial decolorization of an azo dye by extracellular

metabolites from Escherichia coli strain NO3. Bioresource technology. 2004; 91(3):243-248.
4. Chang JS, Chou C, Lin YC, Lin PJ, Ho JY, Hu TL *et al*. Kinetic characteristics of bacterial azo-dye decolorization by Pseudomonas luteola. Water research. 2001; 35(12):2841-2850.
5. Chung KT, Cerniglia CE. Mutagenicity of azo dyes: structure-activity relationships. Mutation Research/ Reviews in Genetic Toxicology. 1992; 277(3):201-220.
6. Dastjerdi R, Montazer M. a review on the application of inorganic nano-structured materials in the modification of textiles: focus on anti-microbial properties. Colloids and surfaces *B:* Biointerfaces. 2010; 79(1):5-18.
7. Dehghani MH, Mahdavi P. Removal of acid 4092 dye from aqueous solution by zinc oxide nanoparticles and ultraviolet irradiation. Desalination and Water Treatment. 2015; 54(12):3464-3469.
8. Dimitrov DS. Interactions of antibody-conjugated nanoparticles with biological surfaces. Colloids and Surfaces A: Physicochemical and Engineering Aspects, 2006, 282-283.
9. Ferraz ERA, Umbuzeiro GA, De-Almeida G, Caloto-Oliveira A, Chequer FMD, Zanoni MVB *et al*. Differential toxicity of Disperse Red 1 and Disperse Red 13 in the Ames test, HepG2 cytotoxicity assay, and Daphnia acute toxicity test. Environmental Toxicology. 2011; 26(5):489-497.
10. Gross M. Travels to the nanoworld: miniature machinery in nature and technology. Plenum Trade, New York, 2001.
11. Jin XC, Liu GQ, Xu ZH, Tao WY. Decolorization of a dye industry effluent by Aspergillus fumigatus XC6. *Applied* microbiology and biotechnology. 2007; 74(1):239-243.
12. Jung R, Steinle D, Anliker R. A compilation of genotoxicity and carcinogenicity data on aromatic aminosulphonic acids. Food and chemical toxicology. 1992; 30(7):635-660.
13. Kim D, El-Shall H, Dennis D, Morey T. Interaction of PLGA nanoparticles with human blood constituents. Colloids and Surfaces B: Biointerfaces. 2005; 40(2):83-91.
14. Meena S, Dipti VAYA, Das BK. Photocatalytic degradation of Malachite Green dye by modified ZnO nanomaterial. Bulletin of Materials Science. 2016; 39(7):1735-1743.
15. Moore MN. Do nanoparticles present ecotoxicological risks for the health of the aquatic environment? Environment international. 2006; 32(8):967-976.
16. Mugdha A, Usha M. Enzymatic treatment of wastewater containing dyestuffs using different delivery systems. Sci Rev Chem Commun. 2012; 2(1):31-40.
17. Rosenkranz HS, Klopman G. The structural basis of the mutagenicity of chemicals in Salmonella typhimirium: The National Toxicology Program data base. Mutation Research/Fundamental and Molecular Mechanisms of Mutagenesis. 1990; 228(1):51-80.
18. Sagar Raut DP, Thorat RT. Green Synthesis of Zinc Oxide (ZnO) Nanoparticles Using Ocimum Tenuiflorum Leaves. International journal of science and research. 2013; 4(5):1225-1228.
19. Sangeetha G, Rajeshwari S, Venckatesh R. Green synthesis of zinc oxide nanoparticles by aloe barbadensis miller leaf extract: Structure and optical properties. Materials Research Bulletin. 2011; 46(12):2560-2566.
20. Sharma NC, Sahi SV, Nath S, Parsons JG, Gardea-Torresde JL, Pal T *et al*. Synthesis of plant-mediated gold nanoparticles and catalytic role of biomatrix-embedded nanomaterials. Environmental science & technology. 2007; 41(14):5137-5142.
21. Singh P, Iyengar L, Pandey A. Bacterial decolorization and degradation of azo dyes. In Microbial degradation of xenobiotics Springer, Berlin, Heidelberg, 2012, 101-133.
22. Stone V, Nowack B, Baun A, van den Brink N, von der Kammer F, Dusinska M *et al*. Nanomaterials for environmental studies: classification, reference material issues, and strategies for physico-chemical characterisation. Science of the total environment. 2010; 408(7):1745-1754.
23. Wang L, Ma W, Xu L, Chen W, Zhu Y, Xu C *et al*. Nanoparticle-based environmental sensors. Materials Science and Engineering: R: Reports. 2010; 70(3-6):265-274.
24. Xu M, Guo J, Cen Y, Zhong X, Cao W, Sun G *et al*. Shewanella decolorationis sp. nov., a dye-decolorizing bacterium isolated from activated sludge of a waste-water treatment plant. International Journal of Systematic and Evolutionary Microbiology. 2005; 55(1):363-368.